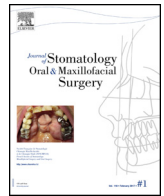




Available online at
ScienceDirect
www.sciencedirect.com

Elsevier Masson France
EM|consulte
www.em-consulte.com/en



Original Article

Comparing “intra operative” tissue engineering strategies for the repair of craniofacial bone defects

V. Hivernaud^{a,b,d,*}, F. Grimaud^{a,b,c,f,1}, J. Guicheux^{a,b,c}, S. Portron^{a,b}, R. Pace^{a,b}, P. Pilet^{a,b,c}, S. Sourice^{a,b}, Wuillem S.^e, H. Bertin^f, R. Roche^d, F. Espitalier^{a,b,c}, P. Weiss^{a,b,c,1}, P. Corre^{a,b,c,f,1}

^a Inserm, UMR-S 1229, R-MeS Lab, Nantes, 44042, France

^b Université de Nantes, UMR-S 1229 R-MeS Lab, UFR odontologie, Nantes, 44042, France

^c CHU de Nantes, PHU 4 OTONN, Nantes, 44042, France

^d STEMCIS, Besançon, France

^e CHU de Nantes, laboratoire d'hématologie, Nantes, 44042, France

^f CHU de Nantes, clinique de stomatologie et chirurgie maxillo-faciale, Nantes, 44042, France

ARTICLE INFO

Article history:

Received 21 September 2018

Accepted 3 January 2019

Keywords:

Tissue engineering

Bone marrow

Stromal vascular fraction

Biphasic calcium phosphate

Nude rat

Calvaria

ABSTRACT

Background: In craniofacial reconstruction, the gold standard procedure for bone regeneration is the autologous bone graft (BG). However, this procedure requiring bone harvesting is a source of morbidity. Bone substitutes, such as biphasic calcium phosphate (BCP), represent an interesting alternative but are not sufficient for bone healing in hypoplastic conditions. In such conditions, osteoprogenitors are essential to provide osteoinduction. Previous studies have shown that BCP associated with total bone marrow (TBM) provides same bone reconstruction as bone graft in a rat model of calvaria defect. Furthermore, adipose tissue stromal vascular fraction (SVF) seems to be another promising source of osteoprogenitor cells that can be used intra-operatively. This study aimed to combine, intra-operative BCP-based bone tissue engineering strategies with TBM or SVF from human sources.

Methods: 5 mm critical-size calvaria defects were performed in 18 nude rat. The defects were filled with intra-operative bone tissue engineering procedures: human BG, human TBM + BCP, human SVF + BCP and, rat TBM + BCP. Animals were sacrificed 8 weeks after implantation and calvaria were processed for histological and radiological examinations. Implanted cells were labelled with a fluorochrome.

Results: Micro-CT analysis revealed partial repair of bone defect. Only hBG significantly succeeded in healing the defect (43.1%). However, low rate of newly formed bone tissue was observed in all tissue engineering conditions (hTBM, hSVF, ratTBM).

Discussion: The lack of bone formation observed in this study could possibly be attributed to the model. **Conclusion:** This study combined with a literature analysis show the stringency of the nude rat calvaria model in term of bone regeneration.

© 2019 Elsevier Masson SAS. All rights reserved.

1. Introduction

Malformations such as facial syndromes, tumors, and facial trauma are clinical situations which may require bone tissue repair at some time in their care. Autologous bone grafting (BG) is considered as the reference procedure [1,2]. However, autologous

bone grafting requires bone harvesting which is still a source of morbidity such as pain or scarring.

For several years, researchers and clinicians have been trying to find an alternative solution to bone grafting with less morbidity. Bone substitutes represent an interesting alternative to autologous bone grafting, mainly in implantology [3] and orthopedic surgery [4]. Among bone substitutes, Biphasic Calcium Phosphate (BCP) has been of particular interest due to its chemical composition and mechanical properties [5,6].

Indeed, BCP are formed with a balance between a stable phase of Hydroxyapatite (HA) and a more soluble phase of Tricalcium phosphate (TCP). The chosen balance between HA and TCP

* Corresponding author at: Inserm, UMR-S 1229, R-MeS Lab, faculté de chirurgie dentaire, 1, place Alexis-Ricordeau, 44042 Nantes, cedex 1, France.

E-mail address: vincent.hivernaud@hotmail.fr (V. Hivernaud).

¹ Authors contributed equally.

influence the release rate of calcium and phosphate ions then influencing bone remodeling.

The results of the implantation of those biomaterials are generally excellent when the recipient site offers good healing conditions [7] which include a small size bone defect, a large blood supply, a rich marrow environment, and adequate skin or mucosa coverage. In contrast, a poorly vascularized recipient site, scarring, hypoplastic or irradiated tissue, will significantly increase the risk of failure [8].

In situations with less than ideal conditions, the osteoconductive properties of BCP are not sufficient to allow a complete healing of the defects. It is thus essential to combine osteoprogenitor cells or osteoinductive molecules with the biomaterial to increase its healing capacity. Mesenchymal Stem Cells (MSC), isolated from several tissues including bone marrow and adipose tissue, have repeatedly shown their interest in bone tissue engineering [9–14]. Among MSC based strategies, seeding the surface of the biomaterial with pre-committed MSCs [15,16] followed by a three-dimensional culture, has shown interesting results both in animal and human models. Nevertheless, this method is complex, has a significant cost, and raises the risk of possible infection during the *in vitro* amplification. In light of these data, and considering the clinical need to substantially simplify potential procedures (i.e., remove *in vitro* culture steps), researchers aimed to develop strategies based on an intra-operative combination of BCP and osteoprogenitors. In a recent study, we have shown that the extemporaneous combination of total fresh rat bone marrow (rat TBM) and BCP yielded results comparable to those obtained with complex MSC based strategies in rat calvaria defects [17].

However, the clinical relevance of those results must be validated with cells of human origins considering the interspecies differences can influence bone regeneration. It is therefore essential to investigate further the potential of human bone marrow cells in a model allowing the use of xenogeneic cells and compare them to the previous strategy which has never been done. Thus, we performed for the first time the pre-clinical evaluation of human TBM in an immunotolerant animal model.

Adipose tissue is another source of osteoprogenitor cells. Like TBM, adipose tissue can be harvested through a simple puncture and can be used extemporaneously, reducing strain on the patient and the surgeon. Numerous studies [18–20] have been conducted on the osteogenic potential of the adipose tissue Stromal Vascular Fraction (SVF), but only few have included BCP in association [21,22]. Despite several studies comparing MSC isolated from those two tissues to date, there is no data on the comparison of SVF and TBM in terms of intra-operative bone regeneration potential.

In order to identify whether intra-operative tissue engineering strategies could be a real alternative to the clinical gold standard, for the first time, this study compared the association of BCP and TBM or SVF from human origin with human bone graft. Those strategies were compared to previously described rat TBM based strategy in a maxillofacial defect of nude rat calvaria.

We hypothesize that the human TBM will give similar results to rat TBM in the previous studies [15,17] and that human SVF cells can achieve at least equivalent bone regeneration than TBM.

2. Materials and methods

2.1. Ethics statement

All human's tissues (bone marrow and adipose tissue) were retrieved according to French National Ethics Committee (DC-2011-1399) and according to Nantes Hospital's biological tissue management protocol (STVO-20141204) after patients gave their informed agreement according to the principles expressed in the Declaration of Helsinki.

Animal study was performed in accordance with European Directive 86/609/CEE for conducting animal experiments, animal care was provided by the Department of Experimental Therapeutics Unit in the University Hospital of Nantes, France. The Ethics Committee of the Nantes University Hospital reviewed and approved the study design (CEEA 2012-250).

2.2. Ceramic particles

Biphasic calcium phosphate particles made of hydroxyapatite (20%) and beta-tri-calcium phosphate (80%) with a size range of 500–1000 μm (MBCP+™) were provided by Biomatlante (Vigneux de Bretagne, France). Eppendorf tubes (Corning, New York, USA) each containing 0.015 g of granules were double packaged and steam sterilized at 121 °C for 20 min before implantation. This granulometry was chosen due to its current use in human clinical practice.

2.3. Animals

The study was performed on eight-week old female nude rats ($n = 18$), provided by a certified breeding center (Charles River, l'Arbresle, France). The animals were acclimatized for one week to the conditions of the local vivarium which was maintained at 24 °C and given a 12 h/12 h light dark cycle. Two female Lewis 1-A rats aged of 7 weeks from the same center were specially designed as rat TBM and Bone Marrow-MSCs (BM-MSC) donors.

3. Total bone marrow and bone graft harvesting

3.1. Rat total bone marrow

Two Lewis-1-A rats were anesthetized using inhaled isoflurane (Foren; Abott, Rungis, France) and sacrificed via intracardiac overdose of sodium thiopental (Nesdonal; Rhône-Merieux, Lyon, France). Rat TBM was isolated from femurs and tibias for extemporaneous grafting and rat BM-MSC isolation. Briefly, the ends of each bone were cut, and 1 mL of rat TBM, mixed with saline, was obtained through an intramedullary bone flush procedure performed with a 26-gauge needle and alpha modified Eagle's medium (α -MEM) (Gibco-Invitrogen Corporation, Saint-Aubin, France). After pooling, half of the rat TBM was used for rat BM-MSC isolation and culture; the other half was seeded on BCP granules 30 minutes before implantation.

3.2. Human total bone marrow and bone graft

Human TBM and BG used in this study came from surgical waste following iliac bone grafting in a 20 years old aged male patient presenting with cleft lip and palate sequel. Collection and implantation of the hTBM and hBG were performed the same day. A part of the hTBM was used for the isolation of hBM-MSCs. Cytology and myelography were performed on this bone marrow.

3.3. Bone marrow mesenchymal stem cells

A portion of the harvested bone marrow from rat and human sources was filtered through a 70 μm nylon mesh filter. The TBM was then seeded in tissue cultured treated polystyrene flasks (Corning, Schiphol-Rijk, Netherlands), and BM-MSCs were isolated based on their adherence capacity after 24 h. Cells were then cultured in proliferative medium (PM₁). Cells were seeded at each passage at 5.10³ cells/cm². The proliferative medium PM₁ was composed of α -MEM supplemented with 2 mM L-Glutamine, 100 U/mL Penicillin/streptomycin and 10% Fetal Bovine Serum

(FBS). BM-MSCs were subsequently incubated at 37 °C in a humidified atmosphere with 5% CO₂ and 95% air. Medium was renewed twice a week until the cells were 80–90% confluent. Cells were then harvested enzymatically from the plastic by an incubation of 4 minutes at 37 °C with 0.25% trypsin Ethylenediaminetetraacetic acid mixture (Invitrogen Corporation, Saint-Aubin, France) and counted using a Malassez hemocytometer and trypan blue exclusion dye. All cells were characterized at the 3rd passage.

3.4. Human stromal vascular fraction

Adipose tissue used in this study came from surgical waste following a liposuction procedure.

Human SVF cells were isolated by collagenase digestion of lipoaspirate obtained from a patient undergoing liposuction as previously described [23]. Briefly, lipoaspirates were digested for 1 h at 37 °C with collagenase (NB4; Serva, Heidelberg, Germany). Digested tissue was then centrifuged at 900 g for 4 min, and the cell pellet (stromal vascular fraction) was washed three times with Ringer Lactate (B Braun Medical), and filtered through a 100 µm Steriflip filter (Millipore, Molsheim, France). After centrifugation, cells were resuspended in a saline solution (Ringer Lactate). Cell number and viability were assessed by cell counting and Trypan blue dye exclusion (Trypan solution 0.02%; Sigma-Aldrich, Saint-Quentin Fallavier, France). Cells were then suspended in Dulbecco's Modified Eagle's medium (DMEM, Gibco-Invitrogen Corporation, Saint-Aubin, France) supplemented with 10% Fetal Bovine Serum (FBS) (PAN-Biotech GmbH, Aidenbach, Germany) and 1% antibiotic (Penicillin/Streptomycin, Life Technologies) and seeded on BCP granules at 18×10^6 cells/cm³ corresponding to 3×10^5 cells/mg of BCP.

To characterize the human SVF (hSVF), a portion of cells was isolated after 24 h of plastic adherence. The non-adhered cells were removed leaving only the attached cells from the hSVF. This population contained adipose derived human stem cells (hASCs). These cells were amplified until the third passage in proliferative medium (PM₂). For hASCs, the PM₂ was made of DMEM medium, 100 U/mL Penicillin/streptomycin and 10% FBS (PAN-Biotech GmbH, Aidenbach, Germany).

3.5. Cell characterization

To demonstrate the in vitro osteogenic differentiation of MSCs from human adipose tissue and human and murine bone marrow, cells were seeded, at 3rd passage, at a density of 1×10^4 cells/cm² and grown in the presence of either proliferative medium (PM) or osteogenic medium (OM) for 28 days. OM was composed of PM supplemented with 10 mM β-glycerophosphate (Calbiochem, Darnstadt, Germany), 0.2 mM sodium L-ascorbate (Sigma-Aldrich, Saint-Quentin Fallavier, France) and 0.1 µM dexamethasone (Sigma-Aldrich, Saint-Quentin Fallavier, France). Cells were incubated at 37 °C in a humidified atmosphere of 5% CO₂ and 95% air, and media were changed every 2–3 days [15].

Calcium deposition was detected after 28 days by Alizarin Red S staining (Sigma-Aldrich, Saint-Quentin Fallavier, France). Briefly,

MSCs were washed with cold phosphate buffered saline (PBS) followed by staining with 2% Alizarin Red S solution for 2 minutes. Stained cells were then extensively washed with deionized water to remove any nonspecific precipitates. Stained layers were visualized with phase contrast microscopy using an inverted microscope (Nikon Eclipse TE 2000 E, Badhoevedorp, Netherlands). Positive red staining indicated the deposition of a calcified matrix on the differentiated cells.

4. Surgical procedure

4.1. Anesthesia and euthanasia protocols

All surgical procedures were performed under general anesthesia using 4% isoflurane inhalation for induction and 2% for preservation. Implants were removed directly after euthanasia by inhalation of carbon dioxide eight weeks after implantation.

4.2. Preparation of the implants

The surgical procedure took place in two phases. Six bone regeneration procedures were tested:

- BCP granules alone (BCP);
- human bone graft (hBG);
- human total bone marrow combined with BCP granules (hTBM + BCP);
- human stromal vascular fraction combined with BCP granules (hSVF + BCP);
- rat total bone marrow combined with BCP granules (rat TBM + BCP) as a positive control of bone repair.
- a negative control condition where defects were left unfilled.

(Table 1) For each strategy, 6 defects were used, corresponding to 18 animals (2 defects per animal). For cellular strategies, cells preparations were left in contact with BCP granules at room temperature during 30 min.

4.3. Creation of the defects

A 1.5 cm longitudinal incision was performed on the head from the front to the neck. Skin and periosteum were retracted to expose the calvaria. A circular critical-sized parietal bone defect (5 mm in diameter) was created bilaterally on each side of the sagittal suture using a circular trephine (Komet Medical, Lemgo, Germany) under infusion of saline solution. Each rat received two randomly assigned implants ($n = 6$ per condition). After grafting, the defects were covered by a pedicle flap isolated from the cervical-occipital muscles to prevent a postoperative migration of the particles. The skin was then closed with absorbable sutures. Immediate postoperative analgesia was provided through a subcutaneous injection of buprenorphine hydrochloride (Buprecare[®] 0.3 mg/mL, 10 µg/kg, Animalcare, Dunnington, UK). The following days, analgesia was provided by acetaminophen orally through a water bottle (0.024% in water).

Table 1

Cells and materials used in the experimental groups.

Experimental condition	Mass of BCP material per implant	Seeding density of cells per mg of BCP	Mass of BG per implant	Volume of TBM per implant
Empty defect	–	–	–	–
BCP	15 mg	–	–	–
hBG	–	–	≈ 15 mg	–
ratTBM + BCP	15 mg	–	–	100 µL
hTBM + BCP	15 mg	–	–	100 µL
hSVF + BCP	15 mg	3.10 ⁴ cells/mg	–	–

4.4. Cell tracking

Fluorochrome CM-DIL (CellTracker™, Invitrogen-Molecular Probes, Eugene, OR, USA) tracked the implanted cells, and marked half of the samples. The fluorochrome was integrated into cell membranes where it is stable for several weeks. The cell labeling was performed by cells incubation with 20 μM of CM-DIL for 5 minutes at 37 °C and then 15 minutes on ice before being mixed with the BCP granules [24]. The resin sections were then analyzed by confocal microscopy on a Nikon Eclipse TE2000-E eC1 confocal laser-scanning microscope (Nikon France) with a laser excitation of wavelength 568 nm.

4.5. Micro computed tomography (μCT) qualitative analysis

Calvaria were imaged postoperatively at 8 weeks by μCT scanning using a high-resolution X-ray μCT system for small animal imaging (SkyScan-1076, Kontich, Belgium). Images were reconstructed and data were analyzed with the manufacturer’s proprietary software (N-Recon, version 1.6.6.0, Skyscan 2011, Kontich, Belgique and CT-Vox, version 2.4.0 r870, Bruker, Kontich, Belgium). This imaging made possible a precise qualitative analysis of defect filling but did not allow a quantitative analysis of bone growth.

4.6. Histological assessment

The explanted bone specimens were fixed for 7 days in a 4% paraformaldehyde in phosphate-buffered saline, and then dehydrated through a graded series of ethanol treatments. After this phase of dehydration, the samples were embedded in glycol methyl methacrylate (GMMA) resin (Sigma-Aldrich, Saint-Quentin Fallavier, France).

For each sample, a cranio-caudal section was performed at the maximal diameter of each implant using a circular diamond saw (SP1600, Leica, Wetzlar, Germany) and serial 5 μm thick sections

were cut using a hard tissue microtome (Polycut SM 2500, Leica, Wetzlar, Germany). The sections were stained with Goldner’s trichrome. New-bone formation, connections with BCP and neighboring tissues, were observed under a light microscope (Axioplan 2, Zeiss, Darmstadt, Germany).

4.7. Scanning electron microscopy

Samples were sanded on a Metaserv 2000 (Buehler, Lake Bluff, USA) then gold-palladium-coated on a Desk III (Denton Vacuum, Moorestown, USA). SEM micrographs were taken using backscattered electrons at 15 kV. The surface of the implant was divided into contiguous high-resolution images, and quantitative evaluation was performed with a semiautomatic image analyzer (Quantimeter 500, Leica, Cambridge, UK). First, the contours of the defects were traced. Areas of newly formed mineralized bone, BCP granules, and non-mineralized tissues were identified by their grey levels and expressed as a percentage of the total defect surface.

4.8. Statistical analysis

Results were expressed as mean ± SEM (Standard Error of the Mean). Results of bone formation in each defect (n = 36) were then compared using a One-Way ANOVA parametric test and a Bonferro-ni’s Multiple Comparison Test. A P-value of less than 0.05 was considered statistically significant.

5. Results

5.1. Bone marrow myelography

A cytological myelographic analysis was performed to assess marrow cell lines, including myeloblasts, myelocytes, proerythroblasts, erythroblasts, megakaryocytes, lymphocytes, plasmocytes,

Table 2
Cytological analysis of the bone marrow. Results are expressed as a percentage of cells per lineage.

Granulocytic lineage					Erythroblastic lineage	Lymphocytes	Plasmocytes	Monocytes	Megacaryocytic lineage
Myeloblastic	Neutrophil promyelocytes	Neutrophil myelocytes	Metamyelocytes	Polynuclears					
5	0.5	11	26.5	29	9	15.5	0	3.5	+

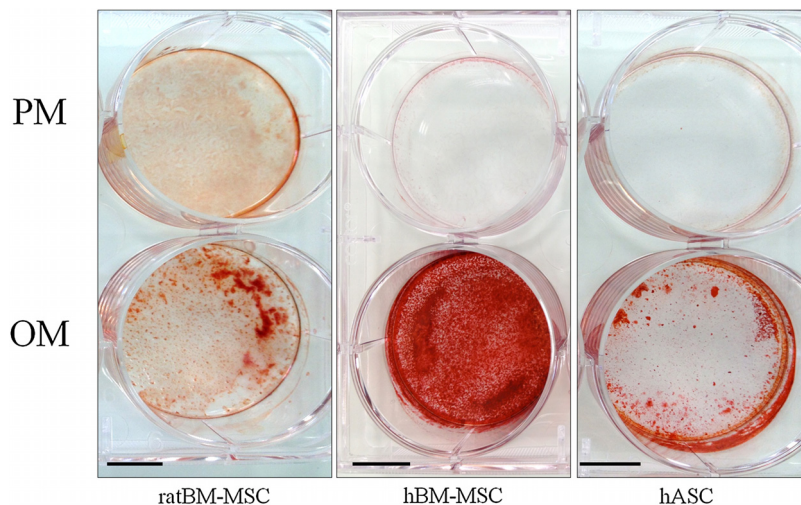


Fig. 1. Osteogenic differentiation of bone marrow- and adipose-derived MSCs. Calcium deposition was investigated by Alizarin Red staining at 28 days. Abbreviations: Mroliferative medium, OM: osteogenic medium, hBM-MSC: mesenchymal stem cells derived from human bone marrow, rat BM-MSC: mesenchymal stem cell derived from rat bone marrow, hASC: mesenchymal stromal cell derived from human adipose tissue. Bar = 1 cm.

and monocytes. The harvested human TBM analysis was within the range of healthy standards (Table 2).

5.2. Cells characterization

The osteogenic potential of rat- and human BM-MSCs and human ASCs (isolated from the implanted TBM and SVF), was evaluated by the mineralization of the extracellular matrix using Alizarin Red staining after 28 days of culture in the presence of PM or OM. Staining of the cell layer was positive for cells isolated from bone marrow and adipose tissue, and cultured in the presence of OM for 28 days (Fig. 1). In contrast, staining was less pronounced for cells grown in the presence of a PM. Between the different MSCs cultured in the osteogenic medium, the more intense staining was present in the hBM-MSCs wells compared with rat BM-MSC and hASC (Table 3).

6. Analysis of new bone formation

6.1. Micro-CT analysis

Three-dimensional μ CT reconstructions confirmed successful implantations and detected failed implantations. Failed implantation was defined as implants in which the BCP granules migrated out of the implant sites. Implantation failures were then excluded from further analyses (1 BCP alone, 1 hTBM + BCP, 1 hSVF + BCP and, 1 rat TBM + BCP). Most of the site were however still filled with implanted granules. In rare cases, isolated granules were partially found at the edge of the created defect.

Micro-CT analysis revealed partial repair of the bone defect implanted with hBG where the hBG remodeled and sometimes fused with the edge of the defect. In contrast, the control defect which contained no BCP showed no closure. BCP-based

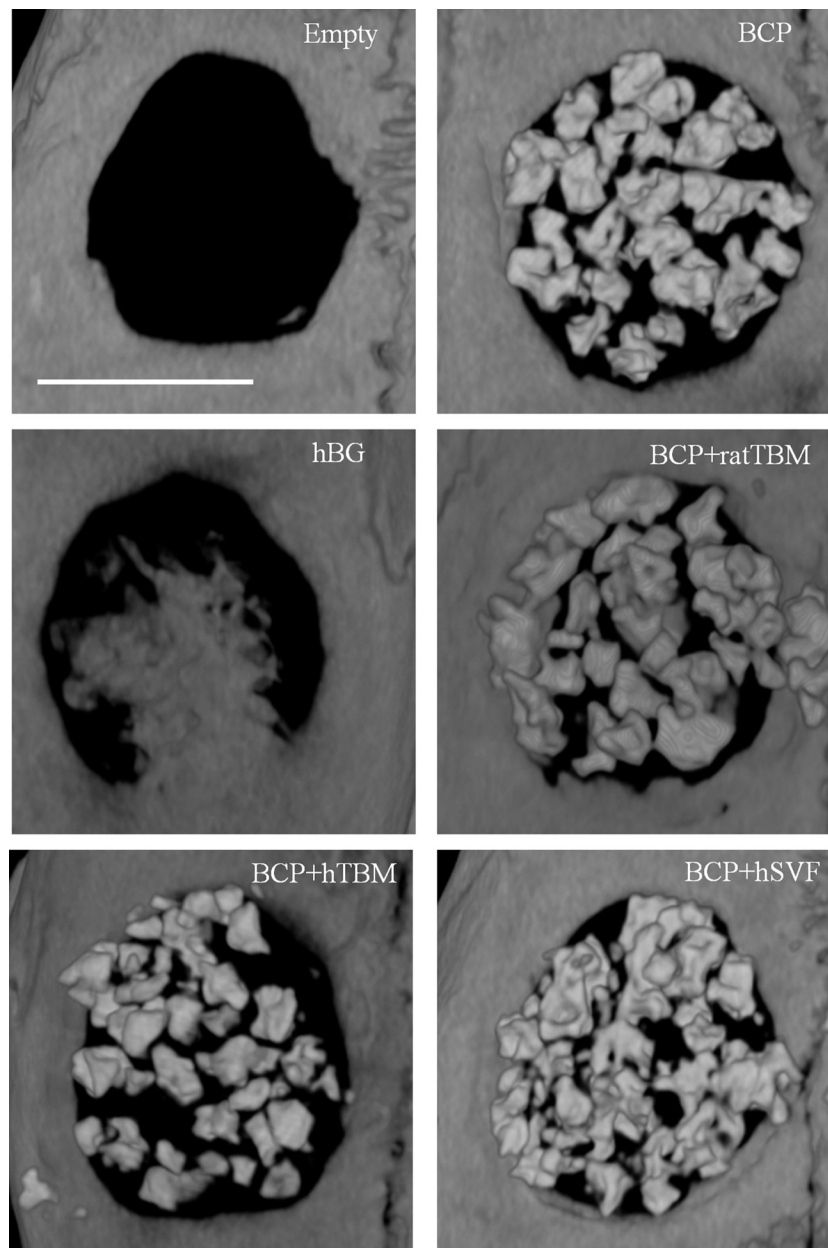


Fig. 2. Three-dimensional reconstruction built from μ CT coronal images at 8 weeks. Three-dimensional reconstructions were built from coronal images for each parietal bone in order to assess the success of the implantation. The results from one representative defect out of six are shown. Abbreviations: hBG: human bone graft, hTBM: human total bone marrow, hSVF: human stromal vascular fraction, rat TBM: rat total bone marrow, BCP: biphasic calcium phosphate. Bar = 5 mm.

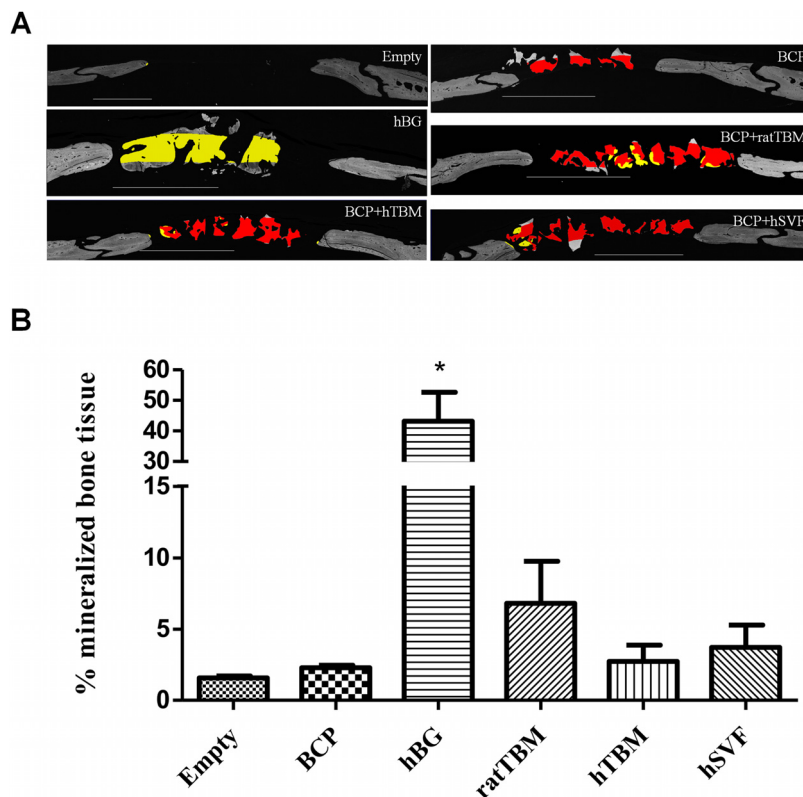


Fig. 3. A. Bone formation scoring at 8 weeks using SEM semi-quantitative analysis. Newly formed bone was assessed by SEM. BCP granules are shown in red, non-calcified tissues in black, native bone in grey, and new bone inside the region of interest in yellow. Bar = 1 mm. B. Quantitative analysis of the bone formation in the defect ($P < 0.05$). Abbreviations: hBG: human bone graft, hTBM: human total bone marrow, hSVF: human adipose tissue stromal vascular fraction, rat TBM: rat total bone marrow, BCP: biphasic calcium phosphate.

conditions revealed non-resorbed granules still presents in the defect (Fig. 2).

6.2. SEM analysis

SEM analysis allowed a qualitative observation of the explants, in particular the interface between newly formed bone and the BCP granules (Fig. 3A), and a quantitative analysis of healing of the defect through the measurement of mineralized bone tissue based on the semi-automatic image analysis. Quantitative and statistical analyses are summarized in Fig. 3B. In our study only hBG significantly succeeded in healing the calvaria defect ($P = 0.0077$). However newly formed bone tissue was observed in tissue engineering conditions with rat TBM, hTBM, and, hSVF.

6.3. Histological analysis

Fig. 4A shows representative histological examples of each condition. Red squares are areas magnified in Fig. 4B.

No inflammatory reaction or encapsulation reaction between the granules and new bone was observed. In the empty control group, there was only a thin layer of fibrous tissue above the dura matter (in red). In the group filled with BCP granules alone, we observed a fibrous tissue surrounding the biomaterials. In the hBG group, we observed a massive filling of the defect with mineralized lamellar bone (LB). In this group, there was also presence of osteocytes like cells (black arrows) suggesting the graft is still composed of living tissue. However, hBG did not always show signs of remodeling and often did not fuse with the edges of the defect (as seen in Fig. 4B). For BCP combined with rat TBM, hTBM or hSVF, cellularized woven bone tissue was present in contact with the granules. However, mineralized lamellar bone

was absent most of the time. In the two groups with human cells (hTBM/hSVF) the presence of red blood vessel-like structure (BV) were commonly seen. The presence of the red staining on blood vessel structures was seen in all the tissue engineering strategies groups.

6.4. Cell tracking

Before implantation, rat and human TBM and human SVF cells were labelled with CM-DIL in half of the defects ($n = 3$). The remaining fluorescence was investigated by fluorescent microscopy after explantation. In all conditions with cells from rat or human origins, signal was present after 8 weeks. Signal could be seen in contact with the BCP, but also in surrounding tissue (Fig. 5). Red signal was converted in white to make it easier to read.

7. Discussion

The aim of this study was to evaluate the bone regenerating potential of BCP combined with hSVF and hTBM. These two intra-operatively isolated MSCs sources could act as an alternative to bone graft which is the current gold standard for bone reconstruction [25]. Previous studies in a syngenic model of rat critical-sized calvaria defect have highlighted the promising use of TBM combined with biphasic calcium phosphate granules [17].

In our study, human TBM, human SVF and rat TBM, all in association with BCP granules, were compared to the current standard (hBG) in a critical-sized calvaria defect in the rat. The use of an immunotolerant animal (NIH-Foxn1 nude) was required, in an attempt to study clinically relevant cell sources of human origin.

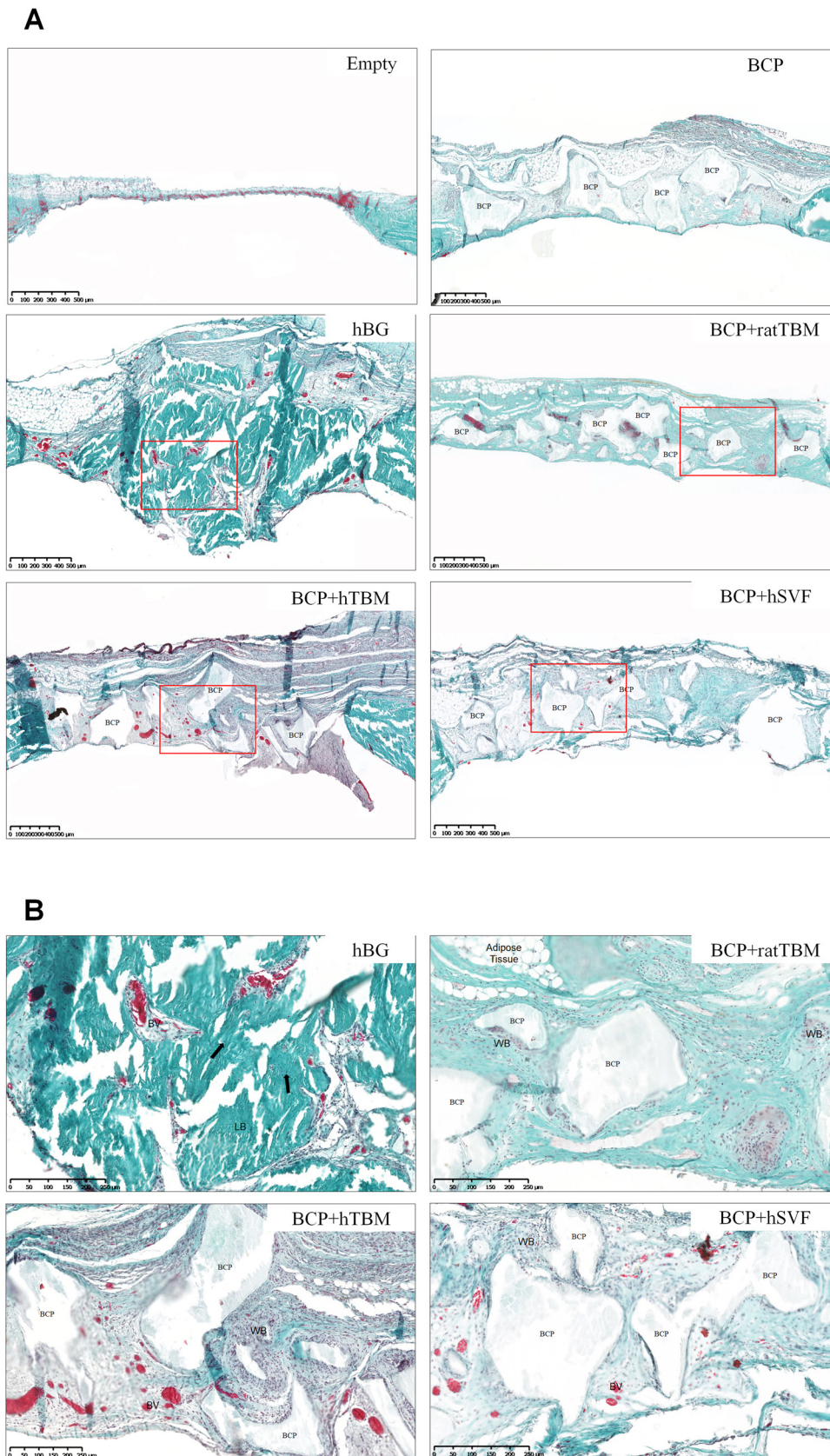


Fig. 4. Histological analysis of bone formation at 8 weeks. Histological study of newly formed tissue was assessed with Goldner Trichrome staining. Mineralized bone is shown in dark green and BCP granules are presented in white. A. Overview of defects histological aspect 8 weeks after implantation. Bar = 500 μ m. B. Magnification of red squares from Fig. 4A. Bar = 250 μ m. Abbreviations: BCP: biphasic calcium phosphate, BV: blood vessel, hBG: human bone graft, hSVF: human stromal vascular fraction, hTBM: human total bone marrow, LB: lamellar bone, rat TBM: rat total bone marrow, WB: woven bone.

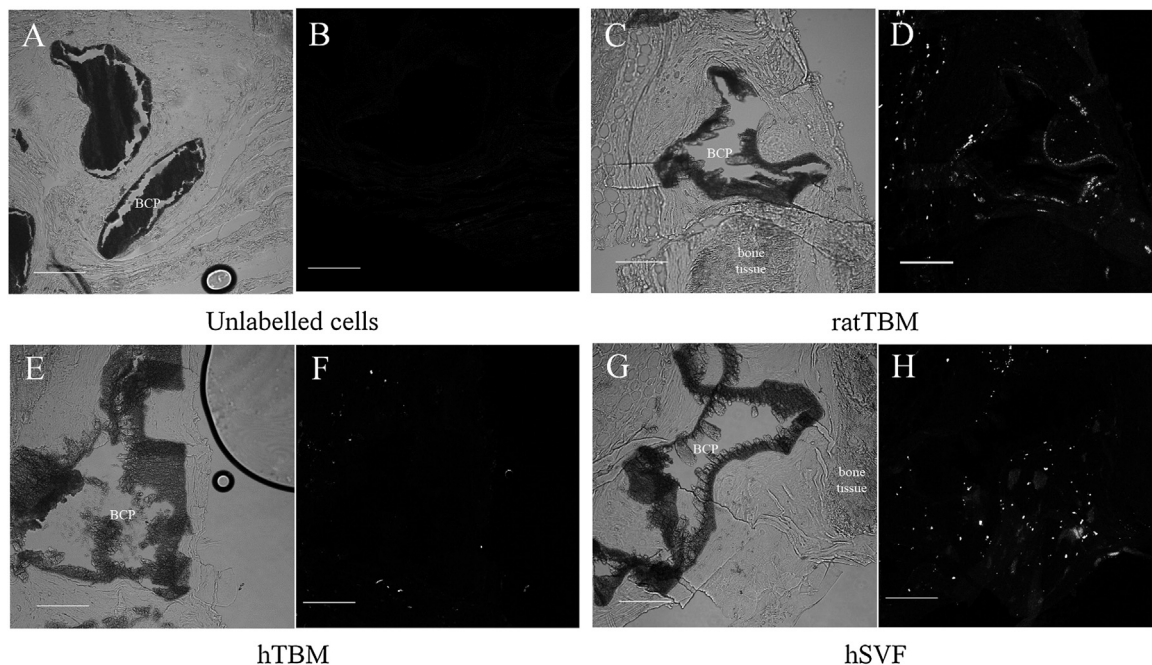


Fig. 5. Fluorescent microscopy at 8 weeks of CM-DIL labelled cells. Cells were labelled with CM-DIL before implantation and observed 8 weeks later. The presence of fluorescence signal was assessed by fluorescent microscopy in transmitted light (A, C, E and, G) then with the red laser 568 nm (B, D, F and, H) in the different tissue engineering conditions. Abbreviations: hTBM: human total bone marrow, rat TBM: rat total bone marrow, hSVF: human stromal vascular fraction. Bar = 100 μ m. Red signal was converted to white to make it easier to read.

The absence of bone regeneration in the empty defect at 8 weeks confirmed that the model we used was a critical-size one. Moreover, the implantation of BCP alone did not produce a significant amount of bone compared to the empty control defect, confirming the lack of osteoinductive properties of BCP alone in hypoplastic bone defects [26].

The bone graft showed the best results in terms of mineralized tissue 8 weeks after implantation with 43.2% of defect filling. The amount of mineralized tissue in this condition was significantly higher than in defect filled with bone tissue engineering procedures. Histological analyses confirmed the presence of living bone containing osteocyte-like cells, partly remodeled. However, it is important to note that the SEM analysis does not allow differentiating implanted bone graft from newly formed bone tissue. Consequently, the percentage of mineralized tissue obtained with the SEM calculation for human bone graft condition might be overstated. In term of defect filling in mineralized tissue the macroscopic images from SEM and histological analyses showed that hBG gave the higher results ($P = 0.0077$). Nevertheless, the same analyses showed several bone graft samples where there was no coalescence between the graft and the edges of the defect, suggesting a low remodeling of the implanted bone compared to our expectation and to previous reports using bone graft [17].

Concerning intra-operative bone tissue engineering strategies with hTBM and hSVF, only little bone formation occurred around the granules. Even though the presence of fluorescence signal could suggest that cells were still present 8 weeks after implantation, the origin of the cells forming the woven bone and the blood vessels could not be determined. The survival of implanted cells in bone defects has already been demonstrated in other models, even though the signal weaken after 2 weeks [27–29]. Woven bone tissue with a fibrous matrix was observable, but no statistically significant mineralized bone formation occurred. There seemed to be a tendency for rat TBM combined with BCP to form more mineralized tissue (6.8%) compared to BCP alone (2.3%) ($P = 0.5476$). Then, the lack of statistical significance could possibly be attributed to a small number of samples.

Several studies have investigated the osteogenic potential of hSVF [4] while only one study tested it in orthotopic model [30]. The ability of hSVF to form bone is still controversial and under debate. Rhee et al. had recorded some osteogenic potential of rat SVF in calvaria defects after 8 weeks using demineralized bone matrix [20], while Müller et al. and Scherberich et al. observed only a slight amount of bone in an ectopic site with hSVF and hydroxyapatite cylinders [21,22]. The present study agrees with these later findings. Thus, some authors have suggested that hSVF's osteogenic potential can be stimulated by adding growth factors or cytokines. However, the use of growth factor in human maxillofacial surgery is debatable as far as adverse effects has been reported, such as inflammatory reactions, graft failure and infections [31,32].

Like SVF, extemporaneous TBM does not require an in vitro culture step, which would make its potential use in the clinical setting much more likely. This technique has rarely been considered for craniofacial bone repair in human [33,34]. In a recent study, rat TBM combined with BCP led to efficient bone formation in calvaria defects similar to bone formation observed in treatments with committed BM-MS-C cultured on BCP granules [17]. To our knowledge, the osteogenic properties of hTBM in hypoplastic bone have yet to be validated. Unexpectedly, in the present study, BCP granules mixed with rat- or hTBM did not demonstrate a significant bone formation. It has been reported that the main limitation of TBM-based strategies is donor-to-donor variability, which cannot be predicted a priori. In our study, rat and human TBM were isolated from only one donor for each experimental condition, which could explain our results. However, a marrow rich in different type of cells was observed in the myelography both for the human patient (Table 1), and the donor rat (data not shown).

In the present study, two human cell sources in combination with BCP granules were compared for the first time in term of bone regeneration strategies: Total Bone Marrow and Stromal Vascular Fraction. Both were previously described as potential cell sources for bone tissue engineering by our team and others. This can be

explained by the fact that TBM and SVF are MSC sources, possess angiogenic properties and can be harvested and used in a one-step procedure. Total Bone Marrow was the first used for bone tissue engineering due to its localization in the bone tissue and the earlier discovery of MSCs. However, SVF is of great interest since the last decade due to its higher concentration in MSCs and its very low harvesting's morbidity. In this study, both hTBM and hSVF gave rise to a limited amount of mineralized tissue after 8 weeks of implantation, even though BM-MSc showed a stronger alizarin red staining than ASC when cultured in the same medium. Then, the assessing of the osteogenic capacities of MSCs *in vitro* was not relevant of the obtained mineralization after implantation. Unfortunately, we were only able to assess one donor for each source of MSC.

The results obtained with rat TBM remain peculiarly disturbing as this strategy was recently evaluated in different autologous bone defect model, including irradiated bone in dog, rat, or rabbit and consistently demonstrated a similar ability to form bone as compared to other strategies [17,35–37]. The major limitation of this study was that only two donors were used in this study. Therefore, there is a risk that observed results could be different with a greater number of human cells donors. However, the same source of rat TBM (Lewis

rats) also gave great results in two other rat calvaria model at 8 weeks, in combination with different bone substitutes or mixed with MSCs (unpublished data). In the later study, the same biomaterial was used making it hard to blame the choice of BCP granules. The granulometry used (500–100 μm) is the one currently used in human clinic and therefore might not be suited to the studied model. However, the same granulometry was used with rat TBM in Lewis rat and resulted in high bone formation [17].

We thus hypothesize that the low rate of mineralized tissue observed in the present study could possibly be attributed to the bone physiology of nude rat model.

To address that hypothesis, a review of the literature concerning that model was conducted. A Pubmed research with the keywords, “nude rat bone” gave 743 results. Among those, 150 concerned bone regeneration studies in the nude rat model. Twenty-six of those studies were using a calvaria defect. A closer look to the previous reported studies is summarized in Table 3 [12,20,38–61].

The previous works in this model used a large variety of biomaterials. The time points of analyses were from one to twelve weeks after defect creation/implantation. Otherwise, we could observe that the higher results in mineralized bone formation rates

Table 3
Literature review of English writing articles using the nude rat model of calvarial defect using PubMed database.

Author/Year	Defect size (diameter)	Implantation time (weeks)	Biomaterial	Use of BMP (or DBM)	% of bone tissue	Histological or Micro-CT evidence of bone formation
Chesmel 1998	8mm	8	DBM	Yes	4.9-6.1% Empty 19.5-28.1% hDBM in gel form 29.4-46.1% Autograft	b
Winn 1999	8mm	2-4	PCL	Yes	22% PLC ~80% PLC/rhBMP2	d
Akita 2004	4mm	2-4-8	Gelatin	Yes	a	b
Kaigler 2006	8.5 mm	6-12	PLGA	No	6% PLGA 33% PLGA/BMSC/EC	d
Acarturk 2006	8mm	2-4-8	DBM	Yes	a	d
Chim 2006	6mm	6	PCL	No	a	b
Shimizu 2007	5 mm	2	a	No	a	b
Yoon 2007	8mm	12	PLGA	No	0% PLGA 72% PLGA + differentiated ASC	c
Roussy 2007	3mm	2-4	PRP/Collagen	No	50% Collagen 45% PRP	b
Mhawi 2007	5 mm					
Qiu 2007	5 mm	4-8	DBM/AM	Yes	32% Empty 84% DBM/AM	d
Park 2008	8mm	8	PGA/PRP	Yes	a	c
Plachokova 2009	8mm	2-4	BCP/PRP	No	14% BCP + PRP 14% BG 18% BG + PRP	c
Rhee 2011	8mm	8	DBM/PLA	Yes	13% Empty 40% DBM 58% DBM + SVF	d
Gardin 2012	5 mm	3	HA	No	a	b
Tremoleda 2012	6mm	1-2	DBM	Yes	a	c
Kim 2012	5 mm	4-8	AM	No	a	d
Ji 2013	8mm	8	PCL/gelatin	No	a	c
Li 2014	5 mm	6	PRF	No	17% Empty 62% L-PRF	d
Annibali 2014	5 mm	2-4-8-12	GDPB/β-TCP	No	a	b
Ma 2014	5 mm	8	Titanium fiber mesh	No	a	c
Choi 2014						
Pippenger 2015	4mm	12	CaP granules + fibrin gel	No	a	c
Suenaga 2015	8mm	8	β-TCP	No	a	d
Wang 2015	8mm	12	CaP cement	Non	11% CPC 30,4% hiPSC-MSc	d
Wang 2015	8mm	12	CaP cement	Yes	22,5% CPC + iPS-MSCs 44,7% CPC + BMP2-iPSMSCs	d

AM: acellular matrix; ADM: acellular human dermal matrix; β-TCP: triCalcium phosphate beta; CaP: calcium phosphate; CPC: calcium phosphate cement; DBM: demineralized bone matrix; EC: endothelial cells; GDPB: granular deProteinized bovine bone; HA: hydroxy apatite; iPSMSCs: induced pluripotent stem cell-derived mesenchymal stem cells; MSC: mesenchymal stem cells; PCLoLyCaproLactone: PGAolyglycolic acid; PLAolyLactic Acid: PLGAoly(Lactic-co-Glycolic) acid, PRPlatelet Rich Plasma; rhBMP2: recombinant human bone morphogenetic protein 2.

Level of evidence based on histological and imaging illustrations.

- ^a No illustrated evidence of bone formation.
- ^b Little evidence of bone formation.
- ^c Slight evidence of bone formation.
- ^d Strong evidence of bone formation.

were obtained while using Demineralized Bone Matrix (DBM) or when other sources of bone morphogenetic proteins were used. Available studies with quantification, computed tomography or histological results, reported a relatively lower bone formation for at 8 weeks when no osteogenic proteins were used. However, some studies evaluating the bone formation at a 12 weeks' time-point reported consequent mineralized tissue formation. It might then be interesting, in the future, to assess our conditions at a 3-months' time-point.

The lack of a competent immune system in these rats could explain the low bone formation rates obtained when no growth factor was used. However, literature results showing higher bone formation rates in non-calvarial defects (i.e. limb bones) suggest that the implication of the immune system in bone formation cannot alone explain this observation.

Those findings from literature and from the present study tend to show that nude rat calvaria defect resembles the situation found in the most hypoplastic cases of maxillofacial bone defects in human where human bone grafts often fail. The nude rat calvaria defect might then be of great interest when assessing these types of afflictions. However, to assess cell-based tissue engineering in such cranio-facial models, a later time point for sacrifice should be recommended.

The use of an immunocompromised model is a limit to extrapolate the obtained results to a real clinical condition considering the immune system of the recipient plays a critical role in the regeneration process. However, the use of animal cells as a model is also limited due to species discrepancies [62]. Tough the use of human cells in an immunocompetent model was also reported to lead to cell deaths and lower bone regeneration [63], leaving a strong dilemma.

As an alternative to nude rat, an immunosuppressive drug in immunocompetent animal could allow the investigation of human cell-based bone tissue engineering for maxillofacial application in less stringent conditions [64]. Although, it would not allow investigating the potential role of the immune system in bone regeneration. To address this issue, the humanized rat model could be used to assess human cells tissue engineering strategies in an "autologous immune" recipient.

8. Conclusion

In conclusion, in this study the bone regenerating potential of human-based intra-operative tissue engineering strategies was evaluated. To assess the osteogenic potential of human SVF and human TBM the nude rat model of calvaria defect was used. In this study, the clinical gold standard of freshly harvested human bone graft was studied and was able to achieve a significant filling of the defect. Those results were in accordance with the conducted literature analysis. The critical-sized calvaria defect is a well-established model to assess the regenerative potential of bone substitute for maxillo-facial applications. However, when it comes to tissue engineering strategies, cells are involved in the regeneration process. The validation of human cells potential is therefore mandatory before clinical applications. To investigate the potential of human cells, an immuno-tolerant model is often selected. In our case, the obtained results highlighted the scarcity of the nude rat calvaria model especially when comparing intra-operative tissue engineering procedures to a clinically relevant positive control.

The investigation of later time points and autologous graft still needs to be done in order to clarify the relevance of this model. Moreover, the lack of statistical results in this study rises the possible need for larger animal groups in future studies on the same model. This model however, seems to match the most

hypotrophic conditions of the maxillofacial bone defects and might not be the best to explore all the craniofacial bone loss applications.

Funding

This work was supported by the association "Les Gueules Cassées". The authors have no financial conflicts of interest.

Disclosure of interest

An author, Vincent Hivernaud received a scholarship grant by the French National Association of Research and Technology and by the STEM CIS company (#2012-1508).

The other authors declare that they have no competing interest.

Acknowledgments

The authors are grateful to Severine Battaglia for μ CT analysis, Caroline Vignes and Greig Couasnay for CM-DIL images and Biomatlante Company for providing the biomaterials. This work was supported the association "Les Gueules Cassées". An author, Vincent Hivernaud received a scholarship grant by the French National Association of Research and Technology and by the STEM CIS company.

References

- [1] Helm GA, Dayoub H, Jane JA. Bone graft substitutes for the promotion of spinal arthrodesis. *Neurosurg Focus* 2001;10(E4):E4.
- [2] Tessier P, Kawamoto H, Matthews D, et al. Autogenous bone grafts and bone substitutes – tools and techniques: I. A 20,000-case experience in maxillofacial and craniofacial surgery. *Plast Reconstr Surg* 2005;116(5 Suppl):6S–24S [discussion 92S–94S].
- [3] Assaf JH, Zanatta FB, de Brito RB, et al. Computed tomographic evaluation of alterations of the buccolingual width of the alveolar ridge after immediate implant placement associated with the use of a synthetic bone substitute. *Int J Oral Maxillofac Implants* 2013;28(3):757–63.
- [4] Cavagna R, Daculsi G, Boulter JM. Macroporous calcium phosphate ceramic: a prospective study of 106 cases in lumbar spinal fusion. *J Long Term Eff Med Implants* 1999;9(4):403–12.
- [5] Le Nihouannen D, Daculsi G, Saffarzadeh A, et al. Ectopic bone formation by microporous calcium phosphate ceramic particles in sheep muscles. *Bone* 2005;36(6):1086–93.
- [6] Miramond T, Corre P, Borget P, et al. Osteoinduction of biphasic calcium phosphate scaffolds in a nude mouse model. *J Biomater Appl* 2014;29(4):595–604.
- [7] Khashan M, Inoue S, Berven SH. Cell based therapies as compared to autologous bone grafts for spinal arthrodesis. *Spine* 2013;38(21):1885–91.
- [8] Corre P, Khonsari RH, Laure B, et al. Synthetic calcium phosphate ceramics in secondary alveoloplasty. *Rev Stomatol Chir Maxillofac* 2012;113(2):131–5.
- [9] Agacayak S, Gulsun B, Ucan MC, et al. Effects of mesenchymal stem cells in critical size bone defect. *Eur Rev Med Pharmacol Sci* 2012;16(5):679–86.
- [10] Arinze TL, Tran T, McAlary J, et al. A comparative study of biphasic calcium phosphate ceramics for human mesenchymal stem-cell-induced bone formation. *Biomaterials* 2005;26(17):3631–8.
- [11] Ben-David D, Kizhner TA, Kohler T, et al. Cell-scaffold transplant of hydrogel seeded with rat bone marrow progenitors for bone regeneration. *J Cranio-Maxillo-fac Surg* 2011;39(5):364–71.
- [12] Kaigler D, Krebsbach PH, Wang Z, et al. Transplanted endothelial cells enhance orthotopic bone regeneration. *J Dent Res* 2006;85(7):633–7.
- [13] Khadka A, Li J, Li Y, et al. Evaluation of hybrid porous biomimetic nano-hydroxyapatite/polyamide 6 and bone marrow-derived stem cell construct in repair of calvarial critical size defect. *J Craniofac Surg* 2011;22(5):1852–8.
- [14] Matsushima A, Kotobuki N, Tadokoro M, et al. In vivo osteogenic capability of human mesenchymal cells cultured on hydroxyapatite and on beta-tricalcium phosphate. *Artif Organs* 2009;33(6):474–81.
- [15] Corre P, Merceron C, Vignes C, et al. Determining a clinically relevant strategy for bone tissue engineering: an "all-in-one" study in nude mice. *PLoS One* 2013;8(12):e81599.
- [16] Mankani MH, Kuznetsov SA, Robey PG. Formation of hematopoietic territories and bone by transplanted human bone marrow stromal cells requires a critical cell density. *Exp Hematol* 2007;35(6):995–1004.
- [17] Corre P, Merceron C, Longis J, et al. Direct comparison of current cell-based and cell-free approaches towards the repair of craniofacial bone defects – a pre-clinical study. *Acta Biomater* 2015;26:306–17.
- [18] Güven S, Mehrkens A, Saxer F, et al. Engineering of large osteogenic grafts with rapid engraftment capacity using mesenchymal and endothelial progenitors from human adipose tissue. *Biomaterials* 2011;32(25):5801–9.

- [19] Kim A, Kim D-H, Song H-R, et al. Repair of rabbit ulna segmental bone defect using freshly isolated adipose-derived stromal vascular fraction. *Cytotherapy* 2012;14(3):296–305.
- [20] Rhee SC, Ji Y-H, Gharibjanian NA, et al. In vivo evaluation of mixtures of uncultured freshly isolated adipose-derived stem cells and demineralized bone matrix for bone regeneration in a rat critically sized calvarial defect model. *Stem Cells Dev* 2011;20(2):233–42.
- [21] Müller AM, Mehrkens A, Schäfer DJ, et al. Towards an intraoperative engineering of osteogenic and vasculogenic grafts from the stromal vascular fraction of human adipose tissue. *Eur Cell Mater* 2010;19:127–35.
- [22] Scherberich A, Galli R, Jaquiere C, et al. Three-dimensional perfusion culture of human adipose tissue-derived endothelial and osteoblastic progenitors generates osteogenic constructs with intrinsic vascularization capacity. *Stem Cells Dayt Ohio* 2007;25(7):1823–9.
- [23] Girard AC, Atlan M, Bencharif K, et al. New insights into lidocaine and adrenaline effects on human adipose stem cells. *Aesthetic Plast Surg* 2013;37(1):144–52.
- [24] Petite H, Viateau V, Bensaïd W, et al. Tissue-engineered bone regeneration. *Nature Biotechnol* 2000;18(9):959–63.
- [25] Rogers GF, Greene AK. Autogenous bone graft: basic science and clinical implications. *J Craniofac Surg* 2012;23(1):323–7.
- [26] Shirasu N, Ueno T, Hirata Y, et al. Bone formation in a rat calvarial defect model after transplanting autogenous bone marrow with beta-tricalcium phosphate. *Acta Histochem* 2010;112(3):270–7.
- [27] Levi B, James AW, Nelson ER, et al. Studies in adipose-derived stromal cells: migration and participation in repair of cranial injury after systemic injection. *Plast Reconstr Surg* 2011;127(3):1130–40.
- [28] Levi B, James AW, Nelson ER, et al. Human adipose derived stromal cells heal critical size mouse calvarial defects. *PLoS One* 2010;5(6):e11177.
- [29] Qi Y, Niu L, Zhao T, et al. Combining mesenchymal stem cell sheets with platelet-rich plasma gel/calcium phosphate particles: a novel strategy to promote bone regeneration. *Stem Cell Res Ther* 2015;6:256.
- [30] James AW, Zara JN, Corselli M, et al. An abundant perivascular source of stem cells for bone tissue engineering. *Stem Cells Trans Med* 2012;1(9):673–84.
- [31] Neovius E, Lemberger M, Docherty Skogh AC, et al. Alveolar bone healing accompanied by severe swelling in cleft children treated with bone morphogenetic protein-2 delivered by hydrogel. *J Plast Reconstr Aesthet Surg* 2013;66(1):37–42.
- [32] Woo EJ. Adverse events reported after the use of recombinant human bone morphogenetic protein 2. *J Oral Maxillofac Surg* 2012;70(4):765–7.
- [33] Warnke PH, Springer IN, Wilfang J, et al. Growth and transplantation of a custom vascularised bone graft in a man. *Lancet* 2004;364(9436):766–70.
- [34] Wongchuensoontorn C, Liebhenschel N, Schwarz U, et al. Application of a new chair-side method for the harvest of mesenchymal stem cells in a patient with nonunion of a fracture of the atrophic mandible – a case report. *J Craniofac Surg* 2009;37(3):155–61.
- [35] Bléry P, Corre P, Malard O, et al. Evaluation of new bone formation in irradiated areas using association of mesenchymal stem cells and total fresh bone marrow mixed with calcium phosphate scaffold. *J Mater Sci Mater Med* 2014;25(25):2711–20.
- [36] Espitalier F, Vinatier C, Lerouxel E, et al. A comparison between bone reconstruction following the use of mesenchymal stem cells and total bone marrow in association with calcium phosphate scaffold in irradiated bone. *Biomaterials* 2009;30(5):763–9.
- [37] Malard O, Guicheux J, Boulter J-M, et al. Calcium phosphate scaffold and bone marrow for bone reconstruction in irradiated area: a dog study. *Bone* 2005;36(2):323–30.
- [38] Acarturk TO, Hollinger JO. Commercially available demineralized bone matrix compositions to regenerate calvarial critical-sized bone defects. *Plast Reconstr Surg* 2006;118(4):862–73.
- [39] Akita S, Fukui M, Nakagawa H, et al. Cranial bone defect healing is accelerated by mesenchymal stem cells induced by coadministration of bone morphogenetic protein-2 and basic fibroblast growth factor. *Wound Repair Regen* 2004;12(2):252–9.
- [40] Annibaldi S, Bellavia D, Ottolenghi L, et al. Micro-CT and PET analysis of bone regeneration induced by biodegradable scaffolds as carriers for dental pulp stem cells in a rat model of calvarial "critical size" defect: preliminary data. *J Biomed Mater Res B Appl Biomater* 2014;102(4):815–25.
- [41] Chesmel KD, Branger J, Wertheim H, et al. Healing response to various forms of human demineralized bone matrix in athymic rat cranial defects. *J Oral Maxillofac Surg* 1998;56(7):857–63 [discussion 864–865].
- [42] Chim H, Schantz JT. Human circulating peripheral blood mononuclear cells for calvarial bone tissue engineering. *Plast Reconstr Surg* 2006;117(2):468–78.
- [43] Choi JW, Park EJ, Shin HS, et al. In vivo differentiation of undifferentiated human adipose tissue-derived mesenchymal stem cells in critical-sized calvarial bone defects. *Ann Plast Surg* 2014;72(2):225–33.
- [44] Gardin C, Bressan E, Ferroni L, et al. In vitro concurrent endothelial and osteogenic commitment of adipose-derived stem cells and their genomics analyses through comparative genomic hybridization array: novel strategies to increase the successful engraftment of tissue-engineered bone grafts. *Stem Cells Dev* 2012;21(5):767–77.
- [45] Ji W, Yang F, Ma J, et al. Incorporation of stromal cell-derived factor-1alpha in PCL/gelatin electrospun membranes for guided bone regeneration. *Biomaterials* 2013;34(3):735–45.
- [46] Kim HJ, Park SS, Oh SY, et al. Effect of acellular dermal matrix as a delivery carrier of adipose-derived mesenchymal stem cells on bone regeneration. *J Biomed Mater Res B Appl Biomater* 2012;100(6):1645–53.
- [47] Li Q, Reed DA, Min L, et al. Lyophilized platelet-rich fibrin (PRF) promotes craniofacial bone regeneration through Runx2. *Int J Mol Sci* 2014;15(5):8509–25.
- [48] Ma J, Both SK, Ji W, et al. Adipose tissue-derived mesenchymal stem cells as monocultures or cocultures with human umbilical vein endothelial cellserformance in vitro and in rat cranial defects. *J Biomed Mater Res A* 2014;102(4):1026–36.
- [49] Mhawi AA, Peel SA, Fok TC, et al. Bone regeneration in athymic calvarial defects with Accell DBM100. *J Craniofac Surg* 2007;18(3):497–503.
- [50] Park EJ, Kim ES, HPE Weber, et al. Improved bone healing by angiogenic factor-enriched platelet-rich plasma and its synergistic enhancement by bone morphogenetic protein-2. *Int J Oral Maxillofac Implants* 2008;23(5):818–26.
- [51] Pippenger BE, Ventura M, Pelttari K, et al. Bone-forming capacity of adult human nasal chondrocytes. *J Cell Mol Med* 2015;19(6):1390–9.
- [52] Plachokova AS, van den Dolder J, van den Beucken JJJ, et al. Bone regenerative properties of rat, goat and human platelet-rich plasma. *Int J Oral Maxillofac Surg* 2009;38(8):861–9.
- [53] Qiu Q-Q, Mendenhall HV, Garlick DS, et al. Evaluation of bone regeneration at critical-sized calvarial defect by DBM/AM composite. *J Biomed Mater Res B Appl Biomater* 2007;81(2):516–23.
- [54] Roussy Y, Bertrand Duchesne MP, Gagnon G. Activation of human platelet-rich plasmas: effect on growth factors release, cell division and in vivo bone formation. *Clin Oral Implants Res* 2007;18(5):639–48.
- [55] Shimizu K, Ito A, Yoshida T, et al. Bone tissue engineering with human mesenchymal stem cell sheets constructed using magnetite nanoparticles and magnetic force. *J Biomed Mater Res B Appl Biomater* 2007;82(2):471–80.
- [56] Suenaga H, Furukawa KS, Suzuki Y, et al. Bone regeneration in calvarial defects in a rat model by implantation of human bone marrow-derived mesenchymal stromal cell spheroids. *J Mater Sci Mater Med* 2015;26(11):254.
- [57] Tremoleda JL, Khan NS, Mann V, et al. Assessment of a pre-clinical model for studying the survival and engraftment of human stem cell derived osteogenic cell populations following orthotopic implantation. *J Musculoskelet Neuronal Interact* 2012;12(4):241–53.
- [58] Wang P, Liu X, Zhao L, et al. Bone tissue engineering via human induced pluripotent, umbilical cord and bone marrow mesenchymal stem cells in rat cranium. *Acta Biomater* 2015;18:236–48.
- [59] Wang P, Song Y, Weir MD, et al. A self-setting iPSCMSC-alginate-calcium phosphate paste for bone tissue engineering. *Dent Mater* 2016;32(2):252–63.
- [60] Winn SR, Schmitt JM, Buck D, et al. Tissue-engineered bone biomimetic to regenerate calvarial critical-sized defects in athymic rats. *J Biomed Mater Res* 1999;45(4):414–21.
- [61] Yoon E, Dhar S, Chun DE, et al. In vivo osteogenic potential of human adipose-derived stem cells/poly lactide-co-glycolic acid constructs for bone regeneration in a rat critical-sized calvarial defect model. *Tissue engineering* 2007;13(3):619–27.
- [62] Prins HJ, Fernandes H, Rozemuller H, et al. Spatial distribution and survival of human and goat mesenchymal stromal cells on hydroxyapatite and beta-tricalcium phosphate. *J Tissue Eng Regen Med* 2016;10(3):233–44.
- [63] Bouvet-Gerbetz S, Boukhechba F, Balaguer T, et al. Adaptive immune response inhibits ectopic mature bone formation induced by BMSCs/BCP/plasma composite in immune-competent mice. *Tissue Eng Part A* 2014;20(21–22):2950–62.
- [64] Espitalier F, Durand N, Remy S, et al. Development of a cyclosporin-A-induced immune tolerant rat model to test marrow allograft cell type effects on bone repair. *Calcif Tissue Int* 2015;96(5):430–7.